Journal of the Nigerian Association of Mathematical Physics
Volume 48 **(***Sept. & Nov., 2018 Issue***), pp219 –226**

THEORETICAL MONITORING OF ENERGY TRANSPORT ON SOLID SURFACES AT NANO-METRIC SCALES

Akande Raphael O.

Theoretical Physics Group, Mountain Top University, Ogun State, Nigeria.

Abstract

The surface is known to intercept energy from bombarding particles. This energy then spreads over the surface. Before now, it has been said that the distribution of this energy landing on the surface is always Gaussian. However, in this paper, the energy distribution patterns on common, simple or ideal, solid surfaces were studied. Flat graphene, cubic and rhombohedral surfaces were studied by indicating the energy leads which transport energy units from one atom to the other, away from the landing site of the bombarding particle. The overall, nano-scale patterns of the entire energy spread on the surfaces suggest a clearly non-Gaussian form. This means the energy distribution on these surfaces cannot be assumed to be uniformly distributed over the surface. The energy travels faster along the length than along the breadth, thus it is anisotropic even on ideal lattice arrangement.

Keywords**:** nano, transport, graphene, cubic, rhombohedral, particles, Gaussian, energy, surface

1. Introduction

Scientific reports, in areas such as nanotherapeutics [1] and surface sputtering, presume a Gaussian distribution on the nano scale range of energy transport. This is not so for all cases, as shown in this paper. The applications of this study can be found in the detection of nano energy shifts from one biological systems to other in radiotherapy and micro/nanodosimetry[2,3]. Also the maximisation of the activities of catalysts in chemical and biochemical reactions [4] and in the development of artificial fire resistant materials [5]. Many atimes there are different degrees of energy absorption on different surfaces. Biological surfaces' energies spread differ from that of the inorganics [6]. This may be due to many factors such as photosynthesis and the likes. Nanotherapeutics is also an application of nano particles/nano energy distribution in biological systems. It is also important that, in drug developments, there is a need to study nano scale energy transport so as to effectively monitor and ensure the delivery of active ingredients and then limit side effects. If the nano energy transport is effectively monitored, as in this paper, much of side effects will be avoided [7]. The metallurgy industry also would require a study of this nano scale energy transport.

The surface is a medium and so it is bound to interact with other media and it is in constant tune with its environment. Due to this interaction, there is a need to master the path of the energy (as given off by the foreign particles interacting with it) in form of a wave through the surface [8]. Earlier mathematical models to study this, in the field of surface sputtering, are the Sigmund's Gaussian method [9] and many other models [10,11]. The Sigmund's Gaussian model is given as:

$$E(r') = \frac{\epsilon}{(2\pi)^{3/2} a b^2} exp\left(-\frac{z'^2}{2a^2} - \frac{x'^2+y'^2}{2b^2}\right) \quad \ldots\ldots\ldots\ldots\ldots\ldots\ldots\ldots\ldots\ldots\ldots\ldots\ldots\ldots\ldots\ldots\ldots\ldots(1)$$

where z' is the distance measured along the ion trajectory and x' and y' are measured in the plane perpendicular to z'. ϵ is the total energy carried by the foreign ion (interacting with the surface) and a, b are the widths of the distribution in the directions parallel and perpendicular to the incoming beams respectively. The energy distribution is Gaussian if $a = b$ and not if $a \neq b$. In this paper, we found that $a \neq b$ at nano-scales [12].

2. Methods

To study this energy transport, the following, listed, assumptions are related and applied in sequential manner to one another. These assumptions were considered as important factors in the energy transport caused by the sputtering process.

1. The spot at which the ions land will be called a sputtered location,
2. The origin of the nano-scale energy transport is from the, delivered, energy spread at the sputtered location,
3. All atoms within the scope of the energy spread are to be regarded as the captured atoms,
4. One could imagine that there are different atomic elements within the captured scope,
5. Ionizations of the captured atoms are caused by the transportation of the energy spread as each atomic elements, within the captured scope, receive different portions of energy,

Corresponding Author**:** Akande R.O., Email: roakande@mtu.edu.ng, Tel: +2348131597032

6. The idea here is to study the variations in the way each atom receives energy and apply the, rapidly changing, PAPCs (Photon Absorption Potential Coefficient as described in [13]) to each atom in the captured space,
7. Due to PAPCs, even the same atoms, but located at different positions, in the sputtered location would be treated differently,
8. Finally, evaluation of the energy of the captured atoms in the, growing, sputtered location is made.

Putting these assumptions together, a many-body equation for the study of the nano-scale transportis developed. This model, which is similar to the Rafil-Tabar Interatomic Potentials [14], majorlyincludes the delivered energy,E_s, the subsequent energies received by the groups of atoms in the, growing, sputtered locations,E_{ji} and the rate of PAPCs as A_r:

2.1 To get the equation for the first set of atoms to receive energy, we have:

$$E_{q11} = E_s - E_s A_{rq11} = E_s(1 - A_{rq11})$$

$$E_{q12} = E_s - E_s A_{rq12} = E_s(1 - A_{rq12})$$

…

for all the first categories:

$$E_{q1i} = E_s(1 - A_{rq11}) + E_s(1 - A_{rq12}) + \cdots$$

$$= E_s[(1 - A_{rq11}) + (1 - A_{rq12}) + \cdots]$$

$$= E_s[N - A_{rq11} + -A_{rq12} - \cdots - A_{rq1N}]$$

$$E_{1i} = E_s \sum_i^N 1 - A_{rq1i} \quad \ldots\ldots \quad (2)$$

2.2 Similarly, to get the equation for the second set of atoms to receive energy, energy of one of the second set of atoms will be given as:

$$E_{q21} = E_s - E_s A_{rq21} + E_s \sum_i^N (1 - A_{rq1i})$$

$$-E_s \sum_i^N (1 - A_{rq1i}) A_{rq21}$$

$$= E_s(1 - A_{rq21}) + (1 - A_{rq21}) E_s \sum_i^N (1 - A_{rq1i})$$

$$= E_s(1 - A_{rq21}) \left\{ 1 + E_s \sum_i^N (1 - A_{rq1i}) \right\}$$

$$= E_s \left\{ 1 + \sum_i^N (1 - A_{rq1i}) - A_{rq21} \sum_i^N (1 - A_{rq1i}) - A_{rq21} \right\}$$

$$= E_s \left\{ 1 - A_{rq21} + (1 - A_{rq21}) \sum_i^N (1 - A_{rq1i}) \right\}$$

for all the second categories:

$$E_{2i} = E_s \left\{ \sum_j^{N_j} (1 - A_{rq2j}) + \sum_j^{N_j} (1 - A_{rq2j}) \sum_i^{N_i} (1 - A_{rq1i}) \right\}$$

$$= E_s \left\{ \sum_j^{N_j} (1 - A_{rq2j}) + \left[1 + \sum_i^{N_i} (1 - A_{rq1i}) \right] \right\} \quad \ldots\ldots \quad (3)$$

2.3 Similarly, to get the equation for the third set of atoms to receive energy, energy of one of the third set of atoms will be given as:

$$E_{q31} = E_s - E_s A_{rq31} + E_s \sum_i^{N_i} (1 - A_{rq1i}) - E_s A_{rq31} \sum_i^{N_i} (1 - A_{rq1i})$$

$$+E_s \left\{ \sum_j^{N_j} (1 - A_{rq2j}) \left[1 + \sum_i^{N_i} (1 - A_{rq1i}) \right] \right\}$$

$$-E_s A_{rq31} \left\{ \sum_j^{N_j} (1 - A_{rq2j}) \left[1 + \sum_i^{N_i} (1 - A_{rq1i}) \right] \right\}$$

$$= E_s(1 - A_{rq31}) + E_s(1 - A_{rq31}) \sum_i^{N_i} (1 - A_{rq1i}) +$$

$$E_s(1 - A_{rq31}) \left\{ \sum_j^{N_j} (1 - A_{rq2j}) \left[1 + \sum_i^{N_i} (1 - A_{rq1i}) \right] \right\}$$

$$= E_s(1 - A_{rq31})\left\{1 + \sum_i^{N_i}(1 - A_{rq1i}) + \sum_j^{N_j}(1 - A_{rq2j})\left[1 + \sum_i^{N_i}(1 - A_{rq1i})\right]\right\}$$

$$= E_s(1 - A_{rq31})\left\{\left[1 + \sum_i^{N_i}(1 - A_{rq1i})\right]\left[1 + \sum_j^{N_j}(1 - A_{rq2j})\right]\right\}$$

for all the third categories:

$$E_{3i} = E_s\sum_k^{N_k}(1 - A_{rq3k}) + E_s\sum_k^{N_k}(1 - A_{rq3k})\sum_i^{N_i}(1 - A_{rq1i})$$

$$E_s\sum_k^{N_k}(1 - A_{rq3k})\sum_j^{N_j}(1 - A_{rq2j})\left(\sum_i^{N_i}(1 - A_{rq1i}) + 1\right)$$

$$= E_s\left\{\sum_k^{N_k}(1 - A_{rq3k})\left\{\sum_j^{N_j}(1 - A_{rq2j})\left[1 + \sum_i^{N_i}(1 - A_{rq1i})\right]\right\}\right.$$

$$\left. + \left[1 + \sum_i^{N_i}(1 - A_{rq1i})\right]\right\} \text{…… …. …. …. …. …. …. …. …. …. …. …. …. …. …. …. (4)}$$

2.4 Similarly, to get the equation for the fourth set of atoms to receive energy, energy of one of the fourth set of atoms will be given as:

$$E_{q41} = E_s - E_sA_{rq41} + E_s\sum_i^{N_i}(1 - A_{rq1i}) - E_sA_{rq41}\sum_i^{N_i}(1 - A_{rq1i})$$

$$+E_s\left\{\sum_j^{N_j}(1 - A_{rq2j})\left[1 + \sum_i^{N_i}(1 - A_{rq1i})\right]\right\}$$

$$-E_sA_{rq41}\left\{\sum_j^{N_j}(1 - A_{rq2j})\left[1 + \sum_i^{N_i}(1 - A_{rq1i})\right]\right\}$$

$$+E_s\left\{\sum_k^{N_k}(1 - A_{rq3k})\{\sum_j^{N_j}(1 - A_{rq2j})\left[1 + \sum_i^{N_i}(1 - A_{rq1i})\right] + \left[1 + \sum_i^{N_i}(1 - A_{rq1i})\right]\}\right\}$$

$$-E_sA_{rq41}\left\{\sum_k^{N_k}(1 - A_{rq3k})\{\sum_j^{N_j}(1 - A_{rq2j})\left[1 + \sum_i^{N_i}(1 - A_{rq1i})\right] + \left[1 + \sum_i^{N_i}(1 - A_{rq1i})\right]\}\right\}$$

$$= E_s(1 - A_{rq41}) + E_s(1 - A_{rq41})\sum_i^{N_i}(1 - A_{rq1i})$$

$$+E_s(1 - A_{rq41})\left\{\sum_j^{N_j}(1 - A_{rq2j})\left[1 + \sum_i^{N_i}(1 - A_{rq1i})\right]\right\}$$

$$+E_s(1 - A_{rq41})\left\{\sum_k^{N_k}(1 - A_{rq3k})\left\{\sum_j^{N_j}(1 - A_{rq2j})\left[1 + \sum_i^{N_i}(1 - A_{rq1i})\right]\right.\right.$$

$$\left.\left. + \left[1 + \sum_i^{N_i}(1 - A_{rq1i})\right]\right\}\right\}$$

for all the fourth categories:

$$E_{4i} = E_s \sum_l^{N_l}\left(1 - A_{rq\,4l}\right)\left\{1 + \sum_i^{N_i}\left(1 - A_{rq\,1i}\right) + \sum_j^{N_j}\left(1 - A_{rq\,2j}\right)\left[1 + \sum_i^{N_i}\left(1 - A_{rq\,1i}\right)\right] + \sum_k^{N_k}\left(1 - A_{rq\,3k}\right)\left\{\sum_j^{N_j}\left(1 - A_{rq\,2j}\right)\left[1 + \sum_i^{N_i}\left(1 - A_{rq\,1i}\right)\right] + \left[1 + \sum_i^{N_i}\left(1 - A_{rq\,1i}\right)\right]\right\}\right\} \quad \text{(5)}$$

In general, we have:

$$E_{nm} = E_s \sum_m^{N_m}\left(1 - A_{rqnm}\right)\left\{1 + \sum_i^{N_i}\left(1 - A_{rq\,1i}\right) + \sum_j^{N_j}\left(1 - A_{rq\,2j}\right)\left[1 + \sum_i^{N_i}\left(1 - A_{rq\,1i}\right)\right] + \sum_k^{N_k}\left(1 - A_{rq\,3k}\right)\left\{\sum_j^{N_j}\left(1 - A_{rq\,2j}\right)\left[1 + \sum_i^{N_i}\left(1 - A_{rq\,1i}\right)\right] + \left[1 + \sum_i^{N_i}\left(1 - A_{rq\,1i}\right)\right]\right\}\right\}$$

$$\cdots$$

$$\sum_m^{N_{m-1}}\left(1 - A_{rq\,3(m-1)}\right)\left\{\sum_m^{N_{m-2}}\left(1 - A_{rq\,2(m-2)}\right) \times \cdots \times \left[1 + \sum_i^{N_i}\left(1 - A_{rq\,1i}\right)\right] + \left[1 + \sum_i^{N_i}\left(1 - A_{rq\,1i}\right)\right]\right\} \quad \text{(6)}$$

All limits of the summation signs are mere dummy variables. Equation (6) is the Photon Potential Difference (PPD) derived to compute the consumption of sputtering energy, landing on the sputtering location, by the atoms in the sputtering location region. In order to employ the electrostatic repulsion of the ionised atoms in explaining the sputtering events, the simulation is carried out by checking, i.e validating, the sum of ionisation energies, I, of all the atoms within the, growing (expanding) sputtering location. Replacing$I$ with the rates of PAPCs, A_R, of the constituent atoms, the validity $\tau$of a sputtering event is given as:

$$\tau = I_{n,m} \leq \partial_{r\,n,m}\left(E_{n,m}\right) \leq I_{n,\mu}$$

$$\tau = A_{r\,n,m} \leq \partial_{r\,n,m}\left(E_{n,m}\right) \leq A_{r\,n,\mu} \quad \text{(7)}$$

$\partial_{r\,n,m}\left(E_{n,m}\right) = \frac{d\bar{v}}{dN_{nr}} \rightarrow \frac{E_{ion}}{N(A_c)}$is the gradual decay of energy as the sputtering location grows.

A_c, thePAPC [13], is given as:

$$A_c = \frac{1}{2z}\left\{ln\left(\frac{1+z^-}{1-z^-}\right) + ln\left(\frac{1+z^+}{1-z^+}\right)\right\} = \frac{1}{2z}\left\{ln\left(\frac{1+z^- + z^+ + z^- z^+}{1-z^- - z^+ + z^- z^+}\right)\right\} \quad \text{(8)}$$

Equation (8) can also be written as:

$$A_c = \frac{1}{z}\{tanh^{-1}(z^-) + tanh^{-1}(z^+)\} \quad \text{(9)}$$

$$z^- = \frac{z_v^-}{|z - z_v^-|} \quad \text{(10)}$$

$$z^+ = \frac{z_v^+}{|z - z_v^+|} \quad \text{(11)}$$

$z^-, z^+$are the extra added and subtracted electrons of the neutral atom in question, respectively. Take for instance, the $A_c$of an atom like $N_a$is will be given as:

for first ionisation, equations (10) and (11) become:

$$z^- = \frac{10}{|11-10|} = 10\,,\ z^+ = \frac{12}{|11-12|} = 12,\ A_c = 0.0167148$$

for second ionisation, we have:

$$z^- = \frac{9}{|11-9|} = 4.5\,,\ z^+ = \frac{13}{|11-13|} = 6.5\,,\ A_c = 0.0346427$$

for third ionisation, we have:

$z^- = \frac{8}{|11-8|} = 2.66667\ ,\ z^+ = \frac{14}{|11-14|} = 4.66667\ ,\ A_c = 0.0556262$

Finally, $A_r = A_c \frac{c}{R}$

where$c$ is the speed of the transported photon and R is the increasing distance of the transporting energy from the landing site of the foreign particle.

2.5Interference of growing sputtering location

Since, equation (6) is for only one sputtered location, there is therefore, need to provide ways to handle the interference of more than one sputtering locations that interfere. This is not to merge isolated sputtering locations but to compute the energy consumption in all the interfering sputtering locations originating from the landing particles. Therefore, each non-interfering sputtering locations are treated, and isolated, differently.

For a sputtering, or sputtered, location the irregular energy flow is given as:

$\beta = \bigcap_{\tau \in A_{n,m<\mu}} \int_n^{n'} \int_m^{m'} \partial_{r\ n,m}\left(E_{n,m,\tau}\right) dmdn$ …… …. …. …. …. …. …. …. …. …. (12)

Equation (12), above, is the extent of energy spread within the validity. The number of captured atoms, expected to be sputtered, is $E_{n,m,\tau}$. It is on these set of atoms that the derived potential, given as equation (6), will be applied. The double integral in equation (12) is to handle the irregular flow of energy in the, growing, sputtered location.

Due to different energies from different ions, landing in such a way that one or more sputtering locations merge, the PPD seems to be from different sources. Therefore, the energy reaching the nm^{th}atoms is given as:

$\beta = \bigcup_{\gamma_{x,y,z}} \sum_{t_o}^{t_{max}} \bigcup_{t^- \le t \le t^+} \left\{ \bigcap_{\tau \in A_{n,m<\mu}} \int_n^{n'} \int_m^{m'} \partial_{r\ n,m}\left(E_{n,m,\tau}\right) dmdn \right\}$ ……. …. …. …. (13)

$\bigcup_{t^- \le t \le t^+}$ is for the possible merger of more than one sputtered locations.$t_o$andt_{max} are the initial and final times of the landing time differences between first ion and the last ion. There could be several ions landing in between this time frame.

$t^+ = t_o^+ + \Delta t\ ,\ \ t^- = t_o^- - \Delta t$ ……. …. …. …. …. …. …. …. …. …. …. …. …. …. …. (14)

For more than two ions:

$$t_o = t_o^+ - t_o^- + \Delta t$$

$t_1 = (t_o^+ - t_o^-) - t_1^- + \Delta t$

$t_2 = [(t_o^+ - t_o^-) - t_1^-] - t_2^- + \Delta t$ ……. …. …. …. …. …. …. …. …. …. …. …. …. …. …. (15)

In general, the time difference between several landing ions:

$t_n = \{\cdots [(t_o^+ - t_o^-) - t_1^-] - t_2^- \cdots - t_{n-1}^-\} - t_n^- + \Delta t$ ……. …. …. …. …. …. …. …. (16)

The quantities $t^-$and $t^+$are designed to help us track the time lapse between any two events. $\Delta t$is the continuously increasing time step for all landing ions. t_o^+andt_o^- are the initial time of any two landing ions and are always increasing. The $+$ and$-$ signs denote the first and next to land respectively. The $\sum_{t_o}^{t_{max}}$ sums up all the landing energies as they land with respect to time. The energy reaching the nm^{th}atom has the time tag to indicate different energies with time. This is because the energy at a first instance would have died down, a bit, before another falls. Therefore, the summation is not the energy that lands but the energy that remains amongst the atoms. The quantity $\bigcup_{\gamma_{x,y,z}}$ is the parameter that records the displaced atoms in the surface for each time frame.

It is important to note that this sputtered location undergoes a form of vibration due to movement of atoms to and fro in the lattice. In order to account for this, seeming error, an assumption that the sputtered location or its constituent atoms behave in a simple harmonic motion manner is made. This assumption is based on the fact that the creation of same charge, around the sputtered location, depends on the number of atoms at that location, the $A_c$of those atoms and the frequency with which the atoms vibrate about their A_c values. This is the most interesting feature of the derived PPD as it helps predict the manner in which the resulting material will react to its environment.

The force of repulsion as the atoms become of the same charge is given as:

$F \propto -\varphi \Rightarrow F = -\sigma\varphi, \quad \sigma = \delta(A_c)$

$m\ddot{\varphi} = F \Rightarrow m\ddot{\varphi} = \delta(A_c)\varphi$

$\ddot{\varphi} + \omega_o^2 \varphi = 0 \Rightarrow \left| \left(\frac{\delta(A_c)}{m} \right)^{1/2} \right|$

$\varphi(A_c, t) = \vartheta \cos(\omega_o t + \rho)$ ……. …. …. …. …. …. …. …. …. …. …. …. …. …. …. (17)

Equation (17) depends on both t and A_c, because both are varying through out the process. $\vartheta$is the geometry of the sputtered location and $\rho$is the number of atoms, possible, in that geometry. However, in this work, the limit of concern is to the distribution of energy only.

3. Results

In this section, the developed model, PPD, is slightly advanced before being applied. The advanced form of PPD is necessitated by considering the fact that the three lattice structures being considered in this work will require different distribution patterns. Hence, acustomised detailed energy transport and pattern of distribution of energy by each atom in the three lattice structures considered. This advanced form assumes that the atoms, on whom an ion lands, are ejected and scattered in every direction in the xy plane and that the z axis is merely a slice of layers of xy planes.

$$\nabla\cdot\varphi^{\lambda}=\left(\underline{i}\frac{\partial}{\partial x}+\underline{j}\frac{\partial}{\partial y}+\underline{k}\frac{\partial}{\partial z}\right)\cdot\left\{\underline{i}a_i^{\lambda}+\underline{j}b_i^{\lambda}+\underline{k}\left[\partial c_i^{\mu v}+\partial d_i^{\mu v}\right]\right\}$$

$$\nabla\cdot\varphi^{\lambda}=\frac{\partial a_i^{\lambda}}{\partial\lambda_x}+\frac{\partial b_i^{\lambda}}{\partial\lambda_y}+\left(\frac{\partial^2 c_i^{\mu v}}{\partial\mu\partial v}+\frac{\partial^2 d_i^{\mu v}}{\partial\mu\partial v}\right)\text{…… …. …. …. …. …. …. …. …. …. …. …. …. (18)}$$

Where i is for the labeling of the four cardinal points and λ is for identifying the sputtered location amongst others. Equation (18) is the energy spread by only one landing ion on a 2D flat surface. The beauty of this equation is that it does not need the angle of landing. Energy just spreads according to the potential describing the landing. Now, for more than one merging ion landing sites, on a 2D flat surface, we have:

$$\nabla\cdot\varphi_j^{\lambda}=\nabla\cdot\left(\varphi_1^{\lambda}+\varphi_2^{\lambda}+\varphi_3^{\lambda}+\cdots+\varphi_n^{\lambda}\right)$$

$$\nabla\cdot\varphi_j^{\lambda}=\sum_j^N\left[\frac{\partial a_{ij}^{\lambda}}{\partial\lambda_x}+\frac{\partial b_{ij}^{\lambda}}{\partial\lambda_y}+\left(\frac{\partial^2 c_{ij}^{\mu v}}{\partial\mu\partial v}+\frac{\partial^2 d_{ij}^{\mu v}}{\partial\mu\partial v}\right)\right]\text{…… …. …. …. …. …. …. …. …. …. …. …. …. (19)}$$

For more than one merging landing ions on a rough 2D flat surface, we simple refer to it as a 3D surface. So we have:

$$\nabla\cdot\nabla\varphi_j^{\lambda}=\nabla\cdot\left(\nabla\left[\varphi_1^{\lambda}+\varphi_2^{\lambda}+\varphi_3^{\lambda}+\cdots+\varphi_n^{\lambda}\right]\right)$$

$$\nabla\cdot\nabla\varphi_j^{\lambda}=\nabla^2\left(\varphi_1^{\lambda}+\varphi_2^{\lambda}+\varphi_3^{\lambda}+\cdots+\varphi_n^{\lambda}\right)$$

$$\nabla^2\varphi_j^{\lambda}=\sum_j^N\left\{\frac{\partial^2 a_{ij\sigma}^{\lambda_x}}{\partial\lambda_x\partial\sigma}+\frac{\partial b_{ij\sigma}^{\lambda_y}}{\partial\lambda_y\partial\sigma}+\left(\frac{\partial^3 c_{ij\sigma}^{\mu v}}{\partial\mu\partial v\partial\sigma}+\frac{\partial^3 d_{ij\sigma}^{\mu v}}{\partial\mu\partial v\partial\sigma}\right)\right\}\text{…… …. …. …. …. …. …. …. …. ….(20)}$$

The interesting thing about this new, advanced, version of the PPD model so far is that it can give us the energy reaching an atom per the type of atom receiving the energy. That is, different atoms placed in the lattice will receive a corresponding energy to its current position. So we have:

$$\nabla^2\varphi_j^{\lambda}=\sum_j^N\left\{\frac{\partial^2 a_{ij\sigma}^{\lambda_x}}{\partial\lambda_x\partial\sigma}A^{nm}+\frac{\partial b_{ij\sigma}^{\lambda_y}}{\partial\lambda_y\partial\sigma}B^{nm}+\left(\frac{\partial^3 c_{ij\sigma}^{\mu v}}{\partial\mu\partial v\partial\sigma}C^{nm}+\frac{\partial^3 d_{ij\sigma}^{\mu v}}{\partial\mu\partial v\partial\sigma}D^{nm}\right)\right\}\text{……. …. …. (21)}$$

Equation (21) describes, in full details, the entire energy spread and the energy reaching each atom in any of the three lattices considered. The different patterns, figures 1 to 6, clearly show that the energy distribution into a material, via its surface, is peculiar to the surface. Variables A^{nm}, B^{nm}, C^{nm} and D^{nm} are the location matrices customizing the different lattice structures into the PPD and are given as follows:

$$A_1^{nm}=\begin{pmatrix}K_{n-(2\lambda_x+1),m,\sigma} & -1\\ K_{n-(2\lambda_x+1),m+1,\sigma} & 1\end{pmatrix}_{i=1}\quad A_2^{nm}=\begin{pmatrix}K_{n,m+(2\lambda_x+3),\sigma} & -1\\ K_{n+1,m+(2\lambda_x+3),\sigma} & 1\end{pmatrix}_{i=2}$$

$$A_3^{nm}=\begin{pmatrix}K_{n+(2\lambda_x+2),m+1,\sigma} & -1\\ K_{n+(2\lambda_x+2),m+2,\sigma} & 1\end{pmatrix}_{i=3}\quad A_4^{nm}=\begin{pmatrix}K_{n,m+2\lambda_x,\sigma} & -1\\ K_{n+1,m+2\lambda_x,\sigma} & 1\end{pmatrix}_{i=4}$$

$$B_1^{nm}=\begin{pmatrix}K_{n-\lambda_x,m+(1-\lambda_x),\sigma} & 0\\ 0 & 1\end{pmatrix}_{i=1}\quad B_2^{nm}=\begin{pmatrix}K_{n-\lambda_x,m+(\lambda_x+2),\sigma} & 0\\ 0 & 1\end{pmatrix}_{i=2}$$

$$B_3^{nm}=\begin{pmatrix}K_{n+(\lambda_x+1),m+(\lambda_x+2),\sigma} & 0\\ 0 & 1\end{pmatrix}_{i=3}\quad B_4^{nm}=\begin{pmatrix}K_{n+(\lambda_x+1),m+(1-\lambda_x),\sigma} & 0\\ 0 & 1\end{pmatrix}_{i=4}$$

$$C_1^{nm}=\begin{pmatrix}K_{n-(2\lambda_x+2)+\mu,m+v,\sigma} & -1\\ K_{n-(2\lambda_x+2)+\mu,m+v,\sigma} & 1\end{pmatrix}_{i=1}\quad C_2^{nm}=\begin{pmatrix}K_{n-(2\lambda_x+2)+\mu,m+(2\lambda_x+2)+v,\sigma} & -1\\ K_{n-(2\lambda_x+2)+\mu,m+(2\lambda_x+3)+v,\sigma} & 1\end{pmatrix}_{i=2}$$

$$C_3^{nm}=\begin{pmatrix}K_{n+(2\lambda_x+3)+\mu,m+(2\lambda_x+2)+v,\sigma} & -1\\ K_{n+(2\lambda_x+3)+\mu,m+(2\lambda_x+3)+v,\sigma} & 1\end{pmatrix}_{i=3}\quad C_4^{nm}=\begin{pmatrix}K_{n+(2\lambda_x+3)+\mu,m+v,\sigma} & -1\\ K_{n+(2\lambda_x+3)+\mu+1+v,m,\sigma} & 1\end{pmatrix}_{i=4}$$

$$D_1^{nm}=\begin{pmatrix}K_{n-1+\mu,m-(2\lambda_x+1)+v,\sigma} & -1\\ K_{n+\mu,m-(2\lambda_x+1)+v,\sigma} & 1\end{pmatrix}_{i=1}\quad D_2^{nm}=\begin{pmatrix}K_{n-1+\mu,m+(2\lambda_x+4)+v,\sigma} & -1\\ K_{n+\mu,m+(2\lambda_x+4)+v,\sigma} & 1\end{pmatrix}_{i=2}$$

$$D_3^{nm}=\begin{pmatrix}K_{n+1+\mu,m+(2\lambda_x+4)+v,\sigma} & -1\\ K_{n+2+\mu,m+(2\lambda_x+4)+v,\sigma} & 1\end{pmatrix}_{i=3}\quad D_4^{nm}=\begin{pmatrix}K_{n+1+\mu,m-(2\lambda_x+1)+v,\sigma} & -1\\ K_{n+2+\mu,m-(2\lambda_x+1)+v,\sigma} & 1\end{pmatrix}_{i=4}$$

$$A^{nm}=\begin{pmatrix}A_1^{nm} & A_2^{nm}\\ A_3^{nm} & A_4^{nm}\end{pmatrix}\quad B^{nm}=\begin{pmatrix}B_1^{nm} & B_2^{nm}\\ B_3^{nm} & B_4^{nm}\end{pmatrix}$$

$$C^{nm}=\begin{pmatrix}C_1^{nm} & C_2^{nm}\\ C_3^{nm} & C_4^{nm}\end{pmatrix}\quad D^{nm}=\begin{pmatrix}D_1^{nm} & D_2^{nm}\\ D_3^{nm} & D_4^{nm}\end{pmatrix}\quad \text{……. …. …. …. …. …. …. …. …. …. (22)}$$

4. Conclusion

The whole essence of this work is to, theoretically, monitor or determine the true flow path of nano-scale energies on a graphene surface and other surfaces mentioned earlier. Having done all the derivations, the goal is achieved. Evaluation of the energy flow of each foreign particle landing on the surface at any time can be done using equation (6) and (22). Determination of the energy flowing away from the sputtered location and the energy reaching each atom along the way can also be done using equation (22) as well. The parameter PAPC has helped to ease the computation by providing us with information about how each different atomic element respond to this energy flow. The PAPC, therefore, helps to determine the eventual path of the energy flow. In essence, for all the surfaces considered and other similar surfaces, there will be a shift from the path of energy flow, as shown in the figures 1 to 6. If the nano energy transport is effectively monitored, both theoretically and experimentally, as achieved in this paper, much of side effects of medical treatments and other similar effects will be avoided or limited. The different patterns, figures 1 and 6, clearly show that the energy distribution into a material, via its

surface, is peculiar to the surface. The current shape and atomic distribution on a surface will define the amount of energy flow into that material and the consequent reaction of the material to its environment. Also, figures 1 to 6 show that the energy transport on a surface is not evenly distributed (at any time) and is therefore, non-Gaussian. The simple reason is that different constituent atoms on the surface, reacting differently to the energy reaching them, will hence determine the future (next) path of the energy flow.
The following figures show the leads (arrows) with which the modeling of the nano-scale energy flow was made:

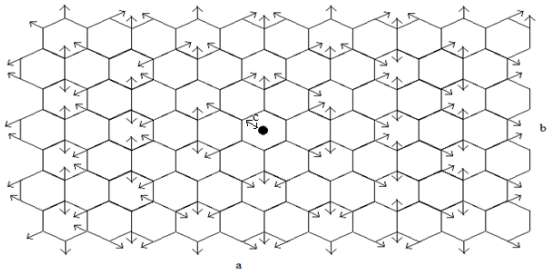

Figure 1: Illustration of an energy distribution from an ion (black dot) landing on an atom (line crossings) on a graphene or hexagonal surface for $c = e$.The side (b) happens to be the slow end while side (a) is the side with faster energy flow. The displayed pattern will shift in correspondence to $c \neq e$.

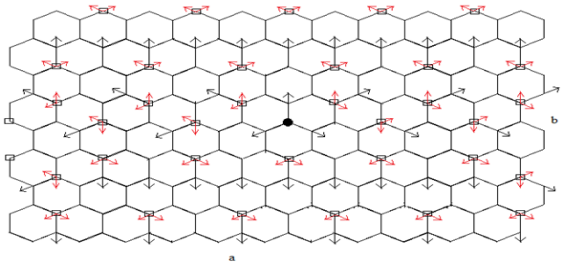

Figure 2: Illustration of an energy distribution from an ion (black dot) landing on an atom (line crossings) on a graphene or hexagonal surface. The side (b) happens to be the slow end while side (a) is the side with faster energy flow. The red lines are the points where the resultant flow is taken.

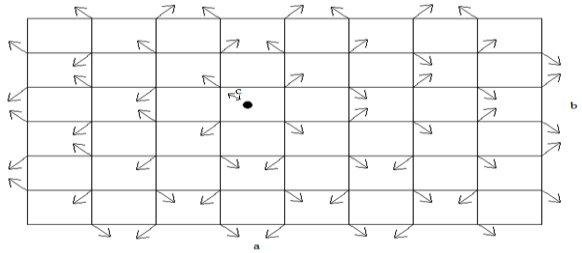

Figure 3: Illustration of an energy distribution from an ion (black dot) landing on an atom (line crossings) on a cubic surface for $c = e$.The side (b) happens to be the slow end while side (a) is the side with faster energy flow. The displayed pattern will shift in correspondence to $c \neq e$.

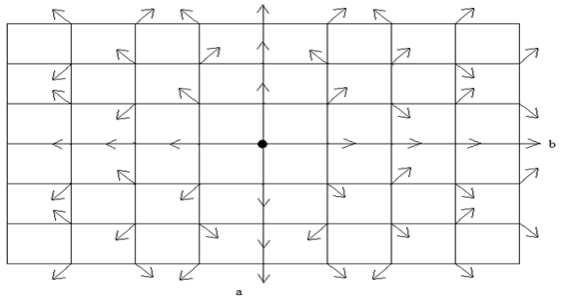

Figure 4: Illustration of an energy distribution from an ion (black dot) landing on an atom (line crossings) on a cubic surface. The side (b) happens to be the slow end while side (a) is the side with faster energy flow.

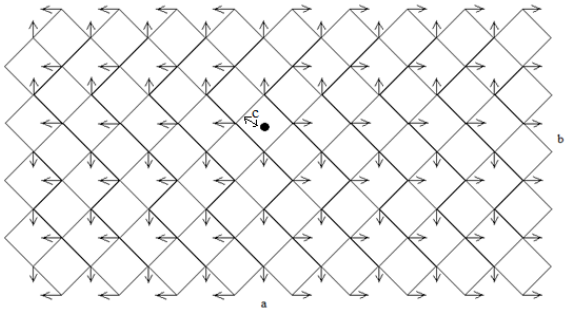

Figure 5: Illustration of an energy distribution from an ion (black dot) landing on an atom (line crossings) on a rhombohedra surface for $c = e$. The side (b) happens to be the slow end while side (a) is the side with faster energy flow. The displayed pattern will shift in correspondence to $c \neq e$.

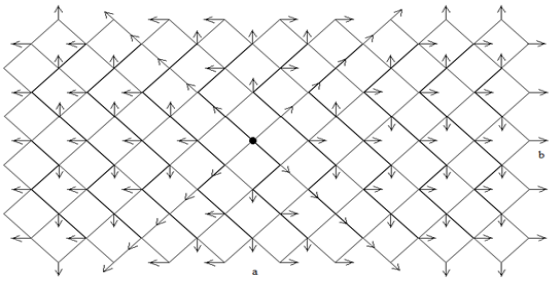

Figure 6: Illustration of an energy distribution from an ion (black dot) landing on an atom (line crossings) on a rhombohedra surface. The side (b) happens to be the slow end while side (a) is the side with faster energy flow.

Reference

[1] Reid Van Lehn et al, Effect of Particle Diameter and Surface Composition on the Spontaneous Fusion of Monolayer-Protected Gold Nanoparticles with Lipid Bilayers, Nano Letters 2013. DOI: 10.1021/nl401365n.

[2] Stepanek J, Blattmann H, Laissue JA, Lyubimova N, Di Michiel M, Slatkin DN., Physics study of microbeam radiation therapy with PSI-version of Monte Carlo code GEANT as a new computational tool. Med Phys. 2000 Jul;27(7):1664-75.

[3] Vanpouille-Box C and Hindré F (2012) Nanovectorized radiotherapy: a new strategy to induce anti-tumor immunity. Front. Oncol. 2:136. doi: 10.3389/fonc.2012.00136

[4] Eric Pop, Energy Dissipation and Transport in Nanoscale Devices. Nano Res (2010) 3: 147-169 DOI 10.1007/s12274-010-1019-z.

[5] Kevin A. Arpin, Mark D. Losego, Andrew N. Cloud, HailongNing, Justin Mallek, Nicholas P. Sergeant, Linxiao Zhu, Zongfu Yu, BerçKalanyan, Gregory N. Parsons, Gregory S. Girolami, John R. Abelson, Shanhui Fan, Paul V. Braun. Three-dimensional self-assembled photonic crystals with high temperature stability for thermal emission modification. Nature Communications, 2013; 4 DOI: 10.1038/ncomms3630.

[6] Dr. Y. rakovich, Alex Rakovich, Energy Transfer at Nano-Bio Interfaces.Photonic group, Trinity Colllege Dublin. http://www.tcd.ie/Physics/photonics/research/biointerface.php

[7] James D. Talton, Ph.D., Co-founder, President and Chief Executive Officer.http://www.nanotherapeutics.com/formulation-development/

[8] Yan Wang, Ajit K. Vallabhaneni, Bo Qiu, and XiulinRuan, TWO-DIMENSIONAL THERMAL TRANSPORT IN GRAPHENE: A REVIEW OF NUMERICAL MODELING STUDIES, Nanoscale and Microscale Thermophysical Engineering, 18: 155–182, 2014. ISSN: 1556-7265 print / 1556-7273 online. DOI: 10.1080/15567265.2014.891680.

[9] Bradley, R. M. and Harper, J. M. E. 1988, Theory of ripple topography induced by ion- bombardment, J VacSciTechnol A, Vol. 6, pp. 2390-2395.

[10] Yewande, O. E., Kree, R and Hartmann, A. K. 2006, Morphological regions and oblique-incidence dot formation in a model of surface sputtering, Phys. Rev. B, Vol. 73, pp. 115434(1)-115434(8).

[11] Yewande, O. E., Kree, R and Hartmann, A. K. 2007, Numerical analysis of quantum dots on off- normal incidence ion sputtered surfaces, Phys. Rev. B, Vol. 75, pp. 155325(1)-155325(8).

[12] Emmanuel O. Yewande, Raphael O. Akande . Topographic phase boundary shifts and Saturation for anisotropic ion straggle during sputter etching.arxiv: 1011.6234v1 [cond-mat.mtrl-sci] 29 Nov 2010. http://arxiv.org/abs/1011.6234

[13] H. Rafil-Tabar, G.A. Mansoori; Interatomic Potential Models for Nanostructures. ISBN: 1-58883-001-2. Encyclopedia of Nanoscience and Nanotechnology. Vol. X pp 1-17.